

Structures of Free-Standing Vertical Thin Films of Hydrophobically Modified Poly(sodium acrylate)s

Frédéric Millet,[†] Jean-Jacques Benattar,[†] and Patrick Perrin^{*,‡}

CEA Saclay, Service de Physique de l'Etat Condensé, F-91191 Gif sur Yvette, Cedex, France, and ESPCI-CNRS-UPMC, UMR 7615, Laboratoire de Physico-chimie des Polymères (LPM), 10, rue Vauquelin, F-75005 Paris, France

Received October 10, 2000; Revised Manuscript Received May 25, 2001

ABSTRACT: Our investigation of free-standing vertical films of hydrophobically modified poly(acrylic acid) sodium salt by the X-ray reflectivity technique shows that the organization of these films strongly depends on the molecular weight and hydrophilic–hydrophobic monomer unit ratio of the copolymers. Long polymer chains with a low amount of hydrophobes form films composed of two layers of coils facing each other. In contrast, short polymer chains with a higher degree of hydrophobic modification form films with a well-defined semioordered structure whose properties are closely linked to the properties of the corresponding solution. We show that this structure is of electrostatic origin. Finally, the comparison of films made of the copolymers in their charged and neutral forms shows that the dominant force within the two types of film is respectively the counterion osmotic pressure and the energy of adsorption of the hydrophobic monomers.

Introduction

Using X-ray reflectivity, we recently reported on the drainage, thickness, and structure of vertical free-standing films of hydrophobically modified poly(acrylic acid) sodium salt (HMPAANA) with moderate to high molecular weights (typically $M_w \geq 34\,000$) and low degree of hydrophobes (<10 mol %).¹ The structure of the films was found to depend on the concentration of the aqueous polyelectrolyte solutions from which the films are drawn, and two concentration regimes were identified. Below the critical aggregate concentration (c_{ac} is the polymer concentration above which intermolecular hydrophobic aggregates form preferentially leading to the formation of a physical 3-D polymer network and hence to a sharp increase of the viscosity of the polymer solution) of the water-soluble associating polyelectrolyte, the film equilibrium thickness varies like the square root of the polymer molecular weight, and it does not depend on either the amount of hydrophobes or the polymer concentration. The thickness is then only controlled by the radius of gyration of the self-screened Gaussian coils formed by the polyelectrolyte chains adsorbed at both air/film interfaces. Above the c_{ac} , the thickness of the films increases rapidly with polymer concentration due to the formation of intermolecular aggregates, and thus it depends strongly on the hydrophobicity of the polymers. Hence, in this concentration regime, the thickness of the film is controlled by the associative properties of the polyelectrolyte. As a consequence, we suggested that a transition from a bimolecular film composed of two monolayers facing each other to a physical microgel occurs at the c_{ac} of the amphiphilic polyelectrolyte. The X-ray reflectivity method, which recently has provided an accurate determination of the structure of Newton black films made of small-molecule surfactants such as sodium dodecyl sulfate² or phospholipids,³ was found not to be sensitive

enough to determine the polymer concentration profile because of the absence of strong electronic density gradients within the polymer films. However, in every polymer films, the presence of a concentrated (about 40% w/w) proximal zone with a thickness of about 25 ± 5 Å was clearly identified in agreement with our observations at the air/water interface.⁴ We also observed that the decrease of the thickness of the films during the drainage is continuous.

In this paper, we extend our investigation to the case of vertical free-standing films made of HMPAANA polyelectrolytes with lower molecular weights and higher degrees of hydrophobic modification. In contrast to longer and less hydrophobic HMPAANA polymers, their thickness does not continuously decrease with time but is quantified. The drainage occurs through successive thickness jumps of equal amplitude. We discuss this observation in the light of recent numerical calculations⁵ and similar experimental results on other polyelectrolyte films.^{6–9} In addition, preliminary results describing the behavior of amphiphilic poly(acrylic acid)s in the neutral form are also reported. We finally compare the magnitude of the adsorption energy of the polyelectrolytes with the monomer and counterion osmotic pressures within the adsorption layer.

Initially, the study of the polyelectrolyte films was aimed at obtaining a better understanding of emulsion stabilization mechanisms by amphiphilic polyelectrolytes on a microscopic scale. It was effectively shown previously that hydrophobically modified poly(sodium acrylate)s are remarkable emulsifiers since they provide both creamed¹⁰ and concentrated¹¹ oil in water emulsions with a good stability. Ordered monodisperse emulsions can also be prepared with these polymeric emulsifiers.^{12–14} Consequently, it is essential to investigate the structure of the polymer films which separate two neighboring droplets and prevent the coalescence. Vertical free-standing films are model systems for these interstitial films, and this paper aims at providing new information about both the adsorption phenomenon and the emulsion stabilization process.

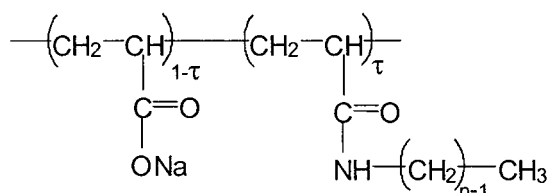
[†] Service de Physique de l'Etat Condensé.

[‡] Laboratoire de Physico-chimie des Polymères (LPM).

* Corresponding author.

Experimental Section

Materials. The synthesis of water-soluble HMPAANA copolymers was detailed previously.^{10,11,15} Poly(acrylic acid) precursor polymers with various molecular weights were supplied by Polysciences. According to our size exclusion chromatography measurements, the weight-average molecular weights (M_w) of the hydrophilic backbone are 5800, 18 000, 34 000, and 120 000. The polydispersity index ranges from 1.2 for the lowest molecular weight to 4 for the highest one. To obtain amphiphilic polymers, *n*-octylamine (C8: the number of carbon atoms is eight) or *n*-dodecylamine (C12) was grafted onto the polymer backbone. The degree of grafting τ (mol %), determined by ¹H NMR spectroscopy and elemental analysis, can easily be controlled during synthesis to adjust the hydrophilic-lipophilic properties of the polymer chains. The name given to the amphiphilic poly(sodium acrylate)s is $M_w \times 10^{-3}(\tau\%)CnNa$ (Na: sodium salt form of the polymer). Five polyelectrolytes, 5.8 25C8Na, 18 20C12Na, 34 10C12Na, 34 1C12Na, and 120 1C12Na, were used in this study. The chemical structures are given by



Aqueous solutions were prepared with double-distilled deionized water with a Milli-Q system (Millipore). The polymer concentrations are given in w/w %. Polymer solutions were stirred gently for 24 h before investigating the film properties. The pH value of the charged polymer solutions is around 8. The viscometric behavior of the aqueous polyelectrolyte solutions is not reinvestigated here since it has already been detailed in the literature.^{1,10} To study the neutral 120 1C12H and 34 1C12H (H for acidic form) polymers, hydrochloric acid (HCl) from a concentrated solution was added to the polyelectrolyte aqueous solutions until the pH of the solution is about 1. The carboxylate groups are then all converted into carboxylic acid groups. Though the addition of hydrochloric acid led to an addition of NaCl into the solution, dialysis was not carried out to eliminate this salt. However, we used the same neutral polymer solutions for the investigation of the films and the bulk viscosity measurements: the interfacial and bulk properties have then been determined under the same salt conditions. All polymers were found to give clear aqueous solutions in the range of the investigated concentrations.

Methods and Equipment. A X-ray reflectivity experiment consists of the measurement of the ratio $R(\theta) = I(\theta)/I_0$ where $I(\theta)$ is the intensity of the specular beam reflected by a surface at an angle θ and I_0 that of the incident beam. The wave vector transfer q is perpendicular to the surface, and the analysis of the reflectivity curves provides information about the mean electron density along the normal z to the surface. The refractive index is given by $n = 1 - \delta - i\beta$, where δ is proportional to the electron density:

$$\delta(z) = \frac{\lambda^2}{2\pi} r_e \rho(z) \quad (1)$$

where λ is the X-ray wavelength, r_e the classical radius of an electron, and $\rho(z)$ the electron density along the z axis. β , which is negligible for organic materials such as polymers, is proportional to the linear absorption coefficient. In fact, we use the original matrix formalism:¹⁶ the system is described as a succession of slabs of constant electron density. The analysis of the reflectivity profile gives the reduced electron density δ , the thickness, and the roughness of each slab.

The main advantage of free-standing films arises from the high electron density gradient at both air-film interfaces. X-ray reflectivity curves display strong Kiessig fringes that

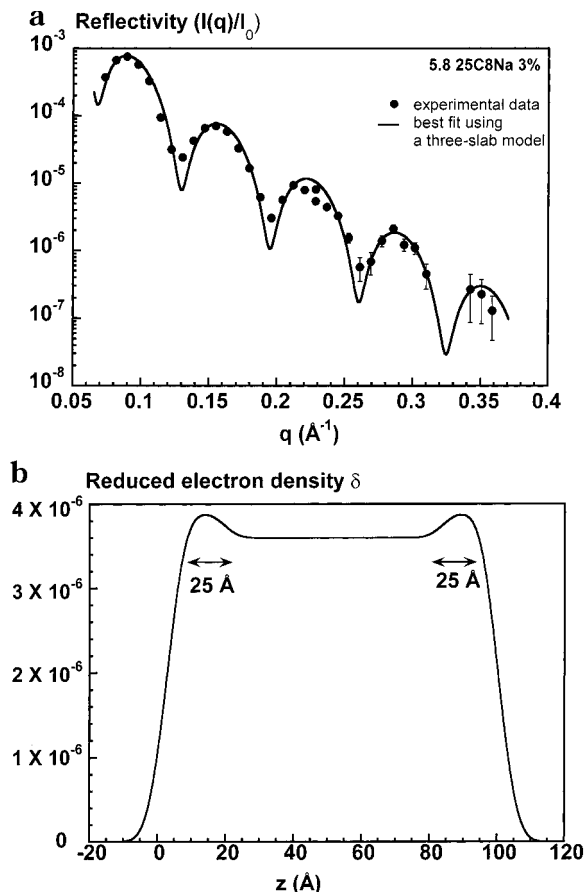


Figure 1. (a) Reflectivity curve ($R(q) = I(q)/I_0$) as a function of the wave vector transfer $q = 4\pi \sin(\theta)/\lambda$ of a film drawn from a 3% concentrated 5.8 25C8Na copolymer solution. (b) Reflectivity profile of the reduced electron density (eq 1) determined from the best fit of the experimental curve (solid line, part a). Two dense layers of adsorbed polymer molecules with a thickness of 25 Å are evidenced.

originate from the interference of the beams reflected on each side of the film whereas reflectivity profiles on the surface of a solution do not exhibit such a contrast. The film drainage can also be followed with a series of reflectivity profiles on a small angle area by choosing a short acquisition period (a few minutes), the film thickness being given by the position of the Kiessig fringes.

Using the experimental method described in detail in previous papers,¹⁻³ films are drawn from the amphiphilic polymer solutions by lifting a vertical metallic frame at constant rate (2 cm/min). Reflectivity experiments are performed using a four-circle diffractometer (Micro-Controle). The X-ray wavelength is $\lambda = 1.5405$ Å (Cu $K\alpha_1$ line), and a small vertical slit (100 μm) placed at a distance of 40 cm from the source ensures a low divergence of the beam (0.15 mrad). A horizontal slit (1.25 mm) limits the height of the illuminated area of the film.

Results and Discussion

Polyelectrolytes with Low Molecular Weights and High Degree of Graftings. We first describe the structure of a film drawn from a 3% concentrated polyelectrolyte (5.8 25C8Na) solution once the drainage is completed. A scan with a long acquisition period (24 h) was performed to obtain an accurate reflectivity profile in order to evidence an electron density gradient. Figure 1a displays the experimental curve (circles). The strong Kiessig fringes arising from the interference of the beams reflected on both sides of the film prove that the parallelism between the two faces of the film is good.

It also clearly appears that, contrary to what has been observed for example with phospholipidic films,³ the shape and the width of the fringes are only weakly modulated, thus indicating that the electron density gradients within the film are weak. However, a single-slab model, corresponding to a homogeneous film, does not provide a suitable fit of the experimental curve. A good fit can only be obtained by introducing two additional slabs (three-slab model) corresponding to dense layers of adsorbed polymer molecules at the air–film interfaces. It is not appropriate to use a five-slab model by adding two other layers corresponding to *n*-octyl grafts emerging from the solution at both air–water interfaces. Because of the shortness of the graft (C8), these last two layers are thin (only a few angstroms). Consequently, they significantly modify neither the electron density profile nor the reflected signal. The reduced electron density profile obtained from the best fit (three-slab model) is given in Figure 1b. To limit the number of fitting parameters, we have considered that the roughness at the air/outer slab and outer slab/film-core interfaces was the same. With this assumption, we determined a value of the roughness equal to 5.5 ± 0.5 Å, slightly larger than that of films consisting of small-molecule surfactants (3.0 ± 0.5 Å) for which the roughness essentially arises from thermal fluctuations.² The best theoretical fit also provides the thickness of the film, 103 ± 1 Å, and the thickness and the reduced electron density of the outer layers, 15 ± 3 Å and $(4 \pm 0.05) \times 10^{-6}$, respectively. The polymer volume fraction ϕ within the outer layers can also be calculated using the following equation:

$$\phi = (\delta - \delta_{\text{water}})/(\delta_{\text{polymer}} - \delta_{\text{water}}) \quad (2)$$

where $\delta_{\text{water}} = 3.56 \times 10^{-6}$, $\delta_{\text{polymer}} = 4.7 \times 10^{-6}$, and $\delta = 4 \times 10^{-6}$ are respectively the reduced electron density of the water, pure polymer, and film outer layers determined from the fit of the experimental curve. Equation 2 leads to a value of $\phi = 40\%$. The reduced electron density of the core of the film, $\delta_{\text{core}} = (3.6 \pm 0.1) \times 10^{-6}$, is equal to that of water within the fitting uncertainty. The central part of the film corresponds to polymer chains extending from the interface to the aqueous sublayer. Within this region, the polymer concentration is low so that the electron density is then close to that of water. So, the structure of the film determined from X-ray reflectivity presents weak electronic density gradients. However, the measurements indicate the presence of two monomer-rich proximal zones and a monomer-poor core domain. Hence, these results are very similar to those obtained for longer polymers with lower degrees of grafting.¹

We now describe the drainage of the films drawn from 5.8 25C8Na solutions at various concentrations. This polyelectrolyte allows the formation of films over almost 2 decades of concentrations. First, it was observed that the drainage is much faster than that for longer polymers.¹ Second, the 5.8 25C8Na copolymer forms films with a well-defined structure revealed by the successive thickness jumps occurring during the drainage. We recall here that the drainage of longer polymers is continuous.¹ Figure 2 gives a schematic picture of the thickness jump phenomenon. The film first remains at a given thickness for periods ranging from a few minutes to several hours (sketch a). At a given moment, a line that is darker to the naked eye than the rest of the film appears at the top of the film (sketch b). This

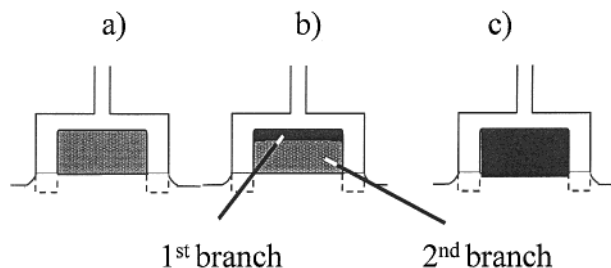


Figure 2. Sketch of the discontinuous drainage of the 5.8 25C8Na copolymer film. A thickness jump is clearly visible to the naked eye.

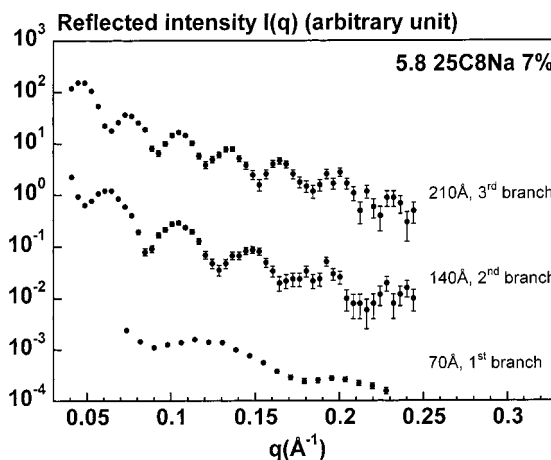


Figure 3. Reflected intensity $I(q)$ of the three successive well-defined thickness of a film drawn from a 7% concentrated 5.8 25C8Na polymer solution. The amplitude of the thickness jumps is 70 Å.

line, which corresponds to a thinner part of the film, progressively extends to finally cover the whole surface of the film (sketch c). The film has then reached a weaker and well-defined thickness through a thickness jump. The X-ray reflectivity curves corresponding to the successive well-defined thickness for a film drawn from a 7% concentrated solution are presented in Figure 3. The amplitude of the thickness jumps is $d = 70$ Å in this particular case. The drainage was thoroughly studied as a function of the polymer concentration. The film thickness is reported in Figure 4 for each polymer solution. Two branches (one thickness jump) are observed at moderate concentrations (between the two vertical dashed lines, region b). In addition, a third branch (or a third series of thickness) appears at high concentrations (region c): as was just mentioned, two thickness jumps of equal amplitude (70 Å) were recorded at a concentration of 7%. Because the film was not stable long enough, we were not able to observe the second jump at a concentration of 10% although we have no doubt that it exists. At low concentrations (region a), no thickness jump is observed so that the film directly reaches its final thickness. It is important to realize that, whatever the concentration, no thickness jump is observed when the film is drawn immediately after pouring the polymer solutions into the trough. Under these conditions, the films drain continuously and stop draining at the thickness given by the first branch. Actually, it is necessary to leave the solutions at rest for 1 h at least to observe the jumps. For the lowest concentration (0.25%), no jump was observed even after leaving the polymer solution at rest for 24 h. With respect to these experimental observations, it seems clear that the jumps are likely to be related to the

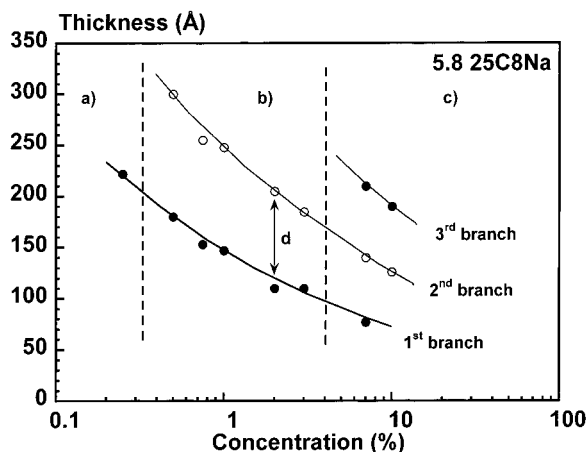


Figure 4. Thickness of the films (± 1 Å) in the whole range of investigated polymer (5.8 25C8Na) concentrations. The number of branches increases with the polymer concentration: one single branch at low concentration (region a), two branches at intermediary concentration (region b), and three branches (corresponding to two thickness jumps of equal amplitude d) at high concentration. For a given branch, the film thickness decreases with increasing concentration.

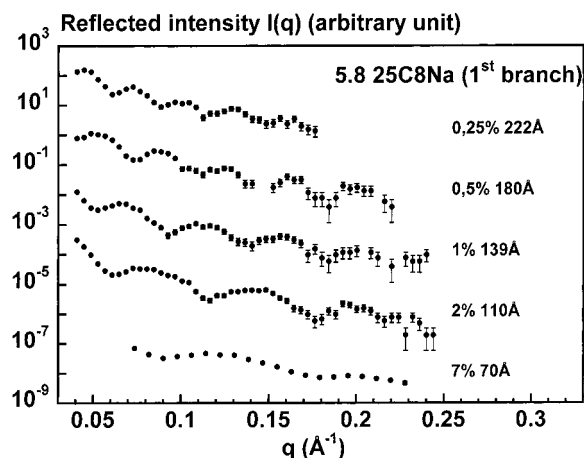


Figure 5. Reflected intensity $I(q)$ corresponding to the first branch over the entire range of 5.8 25C8Na polymer concentrations.

subphase, which needs time to reach a certain level of organization. The reflectivity curves corresponding to the first branch over the entire range of concentrations (0.25–7%) are presented in Figure 5. This branch gives the thickness of the film at the end of the drainage.

The appearance of a third branch at high concentration is of considerable importance for the determination of the origin of the thickness jumps. As a matter of fact, the presence of more than one single jump indicates that the jumps do not originate from binding effects for which only one jump is expected.^{17–21} The same remark holds in the case of two adsorbed polymer layers which interact to protect themselves from bad solvent conditions.²² Finally, the observed phenomenon bears no relation with the thickness jumps encountered with ionic surfactants during the first-order transition from the common black film to the Newton black film^{2,3} described by the DLVO theory.^{23,24} As discussed below, the presence of two jumps is more likely to reveal oscillations in the concentration profile resulting from a stratified organization of the polyelectrolyte chains within the film. This type of behavior has already been observed by disjoining pressure measurements on poly-

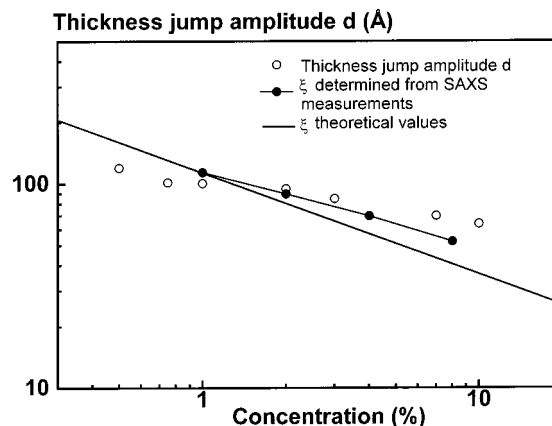


Figure 6. Variation of the thickness jumps amplitude d (± 2 Å) and the experimental and theoretical mesh size values ξ with the polymer concentration c . The experimental ξ values are determined from SAXS measurements on unmodified polymer bulk solutions.²⁸ The theoretical values are calculated from refs 25 and 26. The decrease of d with c is slightly slower than the decrease of both theoretical and experimental ξ values.

electrolyte films. A stratified organization has been observed on mixed films composed of a cationic surfactant (dodecyltrimethylammonium bromide, DTAB) and a charged polymer like poly(styrenesulfonate) (PSS),⁸ acrylamide–acrylamidesulfonate (AM–AMS),⁸ or acrylamide/acrylamidomethylpropanesulfonate (AM/AMPS).^{6,7} The same observation has been made on neutral films of dodecyl hexa(ethylene oxide) (C12E6) containing a semidilute solution of negatively charged poly(styrenesulfonate) (PSS).⁹ In all these references, the measured amplitude of the thickness jumps scales like $c^{-1/2}$ (c being the polymer concentration), which is the scaling of the mesh size ξ of the semidilute polyelectrolyte solutions. For a semidilute solution, the mesh size is the size of a cell unit formed by the polymer lattice. Moreover, the measured values of the amplitude are in good agreement with the theoretical ξ values.^{25–27} In addition, the essential role played by the electrostatic interactions between the monomers is pointed out by the authors who observed the disappearance of the thickness jumps either in the presence of an excess of salt or by replacing the polyelectrolytes by neutral polymers. Finally, the authors report that the number of jumps increases with polymer concentration. We observe the same phenomenon (Figure 4). In light of the above remarks, we plotted the dependence of the thickness jump amplitude d on the amphiphilic polyelectrolyte (5.8 25C8Na) concentration (open circles, Figure 6). The mesh size values of the semidilute unmodified poly(sodium acrylate)s solutions determined from small-angle X-ray scattering (SAXS) measurements by Petit et al.²⁸ are also reported (filled circles). The line corresponds to the theoretical values calculated using the following equation:^{25,26,29}

$$\xi/a = (a/p^2 l)^{1/6} (a^3 c)^{-1/2} \quad (3)$$

where $a = 2.5$ Å is the monomer length, l is the Bjerrum length defined by $l = e^2/4\pi\epsilon kT = 7$ Å in water, and p is the fraction of free counterions. According to the Manning counterion condensation theory,³⁰ $p = a/l - 1/3$ in our case. Equation 3 then becomes $\xi/a = 1.2(a^3 c)^{-1/2}$. The SAXS measurements gave a weaker dependence of ξ on c ($c^{-0.4}$, filled circles) than the theoretical prediction

($c^{-0.5}$). The measured thickness jumps (open circles) follow an even weaker dependence ($c^{-0.3}$), but the values are close to the mesh size values measured by SAXS and are in good agreement with the theoretical calculations for concentrations up to 1%. Hence, it appears that the jumps are actually related to the bulk properties of the semidilute polyelectrolyte solutions. Within this concentration regime, the electrostatic interactions between monomers create a short-range order on the scale of the mesh size of the solution. The charged chains thus seem to be preferentially located in planes parallel to the surfaces of the film, thereby forming a semioordered structure with an oscillating concentration profile, the oscillation wavelength being of the order of ξ . It also explains, at least from a semiquantitative point of view, why a unique thickness was observed for the film drawn from the 0.25% concentrated solutions. In the dilute regime (below the critical overlap concentration c^*), the correlation between the polymer chains is lost, and a continuous drainage would be expected. In pure water, polyelectrolyte chains are stretched out in the dilute regime. Consequently, the critical overlap concentration c^* is usually low, and the dilute regime is difficult to investigate experimentally. However, the 5.8 25C8Na is a short polymer (number of monomer = $N = 60$) so that the concentration c^* can eventually be observed. The equation^{25,29}

$$c^* = (a/p^2 l)(1/a^3 N^2) = 3/a^3 N^2 \quad (4)$$

gives $c^* = 0.45\%$. This value is in good agreement with the value of concentration at which the thickness jumps appear (between 0.25% and 0.5%).

The main property of the polymer solutions is that the mesh size ξ of semidilute polyelectrolyte solutions is independent of the molecular weight of the chains. It was thus essential to investigate the film behavior of HMPAANA copolymers with various molecular weights. As shown previously,¹ the drainage of long polymer films is continuous. For this reason, we chose polymers (the 18 20C12Na and the 34 10C12Na) with intermediate molecular weights. For both polyelectrolyte surfactants, thickness jumps were observed during the drainage. At a concentration of 2%, the thickness jump amplitude for the 18 20C12Na is equal to 95 ± 1 Å. For a 3% concentrated 34 10C12Na solution, the value of the jump is 87 ± 1 Å. The values agree well with our data on the films of 5.8 25C8Na for which the thickness jumps are 95 ± 1 and 85 ± 1 Å at concentrations of 2 and 3%, respectively. The results show that there exists a well-defined structure within the films of HMPAANA copolymers provided that the molecular weight is equal to or lower than 34 000, the oscillation wavelength being independent of the molecular weight and of the order of the mesh size ξ . This feature tends to show that the behavior of the films is linked to the bulk properties of the semidilute solutions from which the films are drawn. Moreover, at first sight, it seems that the amount of grafts does not affect the amplitude of the thickness jumps.

To test the electrostatic origin of the film structure, the behavior of the 5.8 25C8Na copolymer films was examined in the presence of various amounts of sodium chloride at a fixed polymer concentration (3% w/w). The thickness of the films was determined for each NaCl aqueous polymer solutions. Figure 7 presents the dependence of the film thickness on the NaCl concentration. At low salt concentrations ($C_s < 2 \times 10^{-3}$ M), the

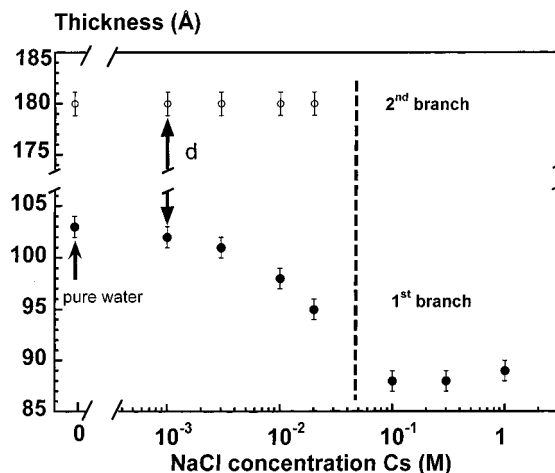


Figure 7. Variation of the thickness with the salt concentration for films drawn from 3% concentrated 5.8 25C8Na copolymer solutions. At high concentrations, the second branch disappears, demonstrating that the thickness jumps originate from electrostatics. The dashed line represents the crossover from the electrostatic regime to the screened regime.

final film thickness (first branch) decreases only slightly with increasing C_s . Between 2×10^{-3} and 10^{-1} M, the thickness decreases from 100 ± 1 to 88 ± 1 Å and levels off for salt concentrations higher than 10^{-1} M. Up to $C_s = 2 \times 10^{-2}$ M, a two-step drainage is observed. As shown in Figure 7, the film first reaches a thickness value equal to 180 ± 1 Å (second branch). For some unexplained reasons, this value does not depend on the salt concentration. In contrast, for concentrations above 10^{-1} M, the film drains directly to its final thickness. The organization of the polyelectrolyte chains and consequently the thickness jumps disappear in the presence of an excess of salt when the electrostatic interactions between monomers are screened. Hence, we have here evidenced that the structure within the film arises from electrostatic interactions. The correlation length of semidilute polyelectrolyte solution in the presence of salt is given by³¹

$$\xi = \xi_0(1 + 2C_s/pc)^{1/4} \quad (5)$$

where ξ_0 is the correlation length in pure water, given by eq 3. This equation expresses that the electrostatic interactions between charged monomers still exist at the mesh scale as long as the electrolyte concentration $2C_s$ does not exceed the counterion concentration pc . In the limit of an excess of salt ($2C_s \gg pc$), ξ scales like $c^{-3/4}$, which is the well-known scaling of the mesh size of semidilute neutral polymer solutions.³² The electrostatic interactions are then screened out on the scale of the mesh size. Conversely, ξ is only slightly modified, and the electrostatic interactions remain within the mesh scale when $2C_s \ll pc$. In the frame of this theory, pc is then the electrolyte concentration corresponding to the transition between both regimes. Assuming that the presence of salt does not alter the condensed counterions/free counterions equilibrium in our experiments, the value of p is constant and equal to $1/3$.³⁰ The theoretical salt concentration required to cross from one regime to the other is $pc/2 = 4 \times 10^{-2}$ M in our case. We find $2 \times 10^{-2} < C_s < 10^{-1}$ (dashed line in Figure 7), which is in reasonable agreement with the theoretical value. So an attempt was made to use eq 5 to describe the dependence of the thickness jump amplitude with

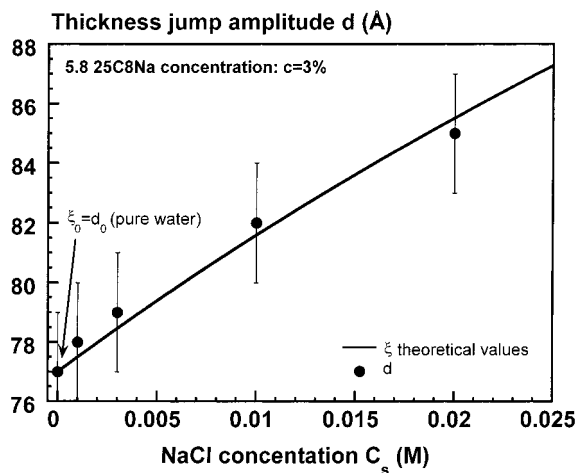


Figure 8. Variation of the thickness jump amplitude d and ξ with the salt concentration in the electrostatic regime. ξ_0 is taken equal to d_0 .

C_s in the range 0–0.2 M. In this analysis, ξ_0 was set equal to d_0 , the thickness jump amplitude in the absence of salt. Figure 8 represents the variation of the amplitude of the thickness jumps d with the salt concentration. The good agreement between the variation of the experimental d values and the theoretical variation of ξ with the salt concentration can be considered as an additional feature, demonstrating the electrostatic origin of the thickness jumps and the semiorordered structure of the films with an oscillating concentration profile, the oscillation wavelength being of the order of ξ .

A slight increase of the correlation length ξ with C_s has already been observed by X-ray scattering on semidilute sodium sulfonate poly(styrene) solutions.³³ At low salinity, a correlation peak, which slightly shifts to lower q values with increasing salt concentration, was observed by the authors. They found that no correlation peak was observed and that the semiorganized structure disappears above a salt concentration roughly equal to the counterion concentration. These experimental results on bulk properties are in a reasonable agreement with eq 5 and qualitatively resemble our results on films.

Charged and Uncharged Polymers with High Molecular Weights and Low Degree of Graftings.

In a previous paper,¹ the behavior of longer polymers with lower amount of hydrophobes was investigated in detail. In particular, we described the behavior of a 120 1C12Na film drawn from a 3% and 6% concentrated polymer salt-free solutions. Once the continuous drainage is completed, a film of about 450 Å was obtained for both concentrations. As mentioned in the Introduction, within this concentration regime, the thickness of the films is controlled by the size of the polymer coil. In what follows, we study a film formed from 2% and 5% concentrated 120 1C12H solutions, that is to say, with the polymer in the neutral acidic form. The preparation of the solutions was given in the Materials section. The drainage is continuous as expected, and for both concentrations, a film thickness of 210 ± 5 Å was measured once it is completed. As for charged polymers, the thickness thus seems to be independent of the concentration. More importantly, the film thickness of the neutral polymer is much smaller than that of the corresponding charged polymer. In the latter, the osmotic pressure of the sodium counterions is responsible

for the formation of thicker films. Hence, it clearly appears that the counterion osmotic pressure is the key parameter that determines the thickness and the structure of the films and is then the dominant contribution to the forces within the HMPAANA polyelectrolyte films. The predominance of this term is the result usually obtained in bulk polyelectrolyte solutions³¹ as well as in dense adsorbed layers of polyelectrolyte chains^{34,35} in the absence of salt. In particular, Pincus showed that the important stretching of polyelectrolyte brushes in contact with a salt-free solution arises from the counterion's osmotic pressure. This theoretical approach was confirmed by the experimental data reported by Gueunoun et al.,³⁶ who studied vertical free-standing films composed of two poly(styrenesulfonate) brushes. To gain a better understanding of the behavior of neutral films, the 34 1C12H polymer films, made from solutions at the same concentrations as for the 120 1C12H, were also investigated. The measured thickness is 180 Å. Hence, the effect of changing the molecular weight of the neutral polymers on the film thickness is weak. To compare interfacial and bulk behaviors of both polymers, we have determined their hydrodynamic radii R_h and their Huggins coefficients K_H by viscosity measurements using the couple of equations:

$$\frac{\eta - \eta_{\text{solvent}}}{\eta_{\text{solvent}} c} = [\eta] + K_H [\eta]^2 c \quad (6a)$$

$$[\eta] = \frac{2.5 N_A}{M_w} \frac{4\pi R_h^3}{3} \quad (6b)$$

where η and η_{solvent} are the solution and solvent viscosity, respectively, and N_A is the Avogadro number. The values of the radii are 31 and 82 Å for the 34 1C12H and 120 1C12H polymers, respectively. The Huggins coefficient K_H , which gives the solvent quality, is equal to 0.4, which is an intermediate value between those corresponding to good ($K_H = 0.3$) and Θ ($K_H = 0.5$) solvent conditions. On one hand, the values of the thickness of both films are close, and on the other hand, the hydrodynamic radii are rather different. Consequently, the thickness of the adsorbed layers is certainly not controlled by the size of the neutral polymer coil as it is the case for homopolymers in weak interactions (lower than kT per monomer) with the surface.²⁵ This model cannot be applied to our systems in which the polymers interact strongly with the surface. Indeed, the interaction of an alkyl chain with the air/water interface increases linearly with the number of CH_2 group of the chain and is $1.25kT$ per CH_2 group. For a dodecyl group, the interaction energy is thus $15kT$. We suggest that the thickness of about 200 Å (180 Å for the 34 1C12H and 210 Å for the 120 1C12H) measured for both polymer films could be due to the formation of a brush stretching perpendicular to the surface between two successive adsorbed grafts (Figure 9). On average, two successive grafts of a polymer chain are separated by 100 monomers of size equal to $a = 2.5$ Å. According to this model, an adsorbed layer thickness of 125 Å is expected. The resulting film thickness (250 Å) of the fully stretched brush is of the same order as the experimental thickness values. More specifically, since the adsorption energy of a sticker ($15kT$ per sticker) is much larger than kT and since the (neutral) monomer osmotic pressure is low in the absence of counterions, most of the dodecyl grafts are possibly adsorbed at the

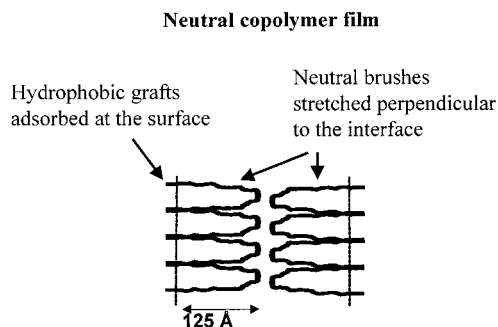


Figure 9. Sketch of neutral copolymer films (34 1C12H and 120 1C12H copolymers). Most of the grafts are adsorbed and the hydrophilic chains between two grafts are stretched perpendicular to the surfaces of the film. The presence of a dense layer near the surfaces and the existence of a monomer concentration profile within the brush should be considered. However, the schematic representation does not take account of these features.

interfaces. This leads to the high-density regime described by the Alexander–de Gennes model³⁷ or more exactly by the Marques–Joanny model.³⁸ In the latter, the authors describe the adsorption of a neutral copolymer, which consists of stickers uniformly distributed along the polymer chains in interaction with the surface, a fraction of which being adsorbed. Between the stickers, the rest of the macromolecules form a brush in good solvent conditions that can be described by the de Gennes–Alexander theory. According to the theoretical model, the thickness of the adsorbed layer (D) is independent of the molecular weight. Combining eqs IV.1 and IV.10 of ref 38 and assuming that all the stickers are adsorbed at the interface, its value is given by the equation

$$D = a\tau^{-3/5}\mu^{2/5} \quad (7)$$

where μ is the interaction energy per sticker in kT units. Our experimental results are in good agreement with this model. First, we have seen that the film thickness varies only slightly with the molecular weight. Second, with $\tau = 1\%$, $a = 2.5$ Å, and $\mu = 15$, we calculate a value of D equal to 117 Å. The theoretical value of the film thickness, 234 Å, compares well with our measurements (180 and 210 Å) taking account of the differences that exist between the experimental and theoretical polymer chains. First, the stickers are randomly and uniformly distributed along the experimental and theoretical polymer backbone, respectively. Second, the polymer molecules considered in the model are in better solvent conditions (good solvent) than the 120 1C12H and 34 1C12H macromolecules, which are in an intermediary state between good and Θ solvent conditions ($K_H = 0.4$). Consequently, the experimental chains are supposed to form a thinner layer than calculated from the model. These two reasons and especially the second one could certainly explain the slight discrepancy observed between the values for experimental and theoretical film thicknesses.

General Behavior of HMPAANA and HMPAAH Films. Whether or not a continuous or a thickness jumps type of drainage is observed upon forming films of HMPAANA polyelectrolyte is an interesting question. According to our experiments, the films exhibit two types of drainage and thus two types of structure depending on both the molecular weight of the precursor polymer and the amount of hydrophobes (Figure 10).

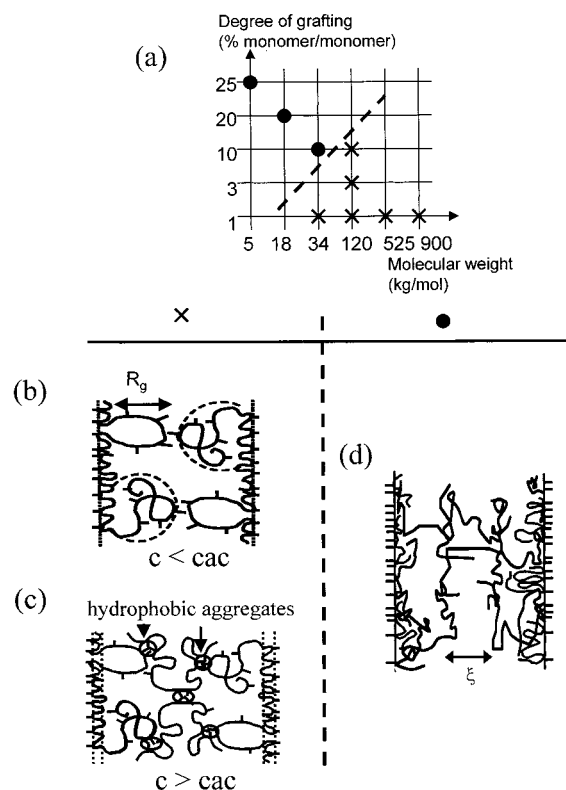


Figure 10. General behavior of the HMPAANA films. (a) The organization of the polymer chains within the films depends on the molecular weight and degree of grafting of the copolymer. Copolymers showing continuous and discontinuous drainage are indicated by the \times and \bullet symbols, respectively. (b) For long chains with low degrees of grafting, the adsorbed molecules form large dangling ends and the thickness of the films is controlled by the radius of gyration (R_g) of the polyelectrolyte chains. (c) Above the critical aggregate concentration (cac), these copolymers form hydrophobic aggregates within the films leading to the formation of a microgel. The thickness of the film increases rapidly with the concentration and it is controlled by the associative properties of the polymer. (d) The semiordered structure is observed for short polymer chains with numerous grafts.

First, the charged copolymers with sufficiently high molecular weights (typically $\geq 34\,000$) and low degree of grafting ($<10\%$) (Figure 10a (\times)) develop large loops and dangling ends below the cac (Figure 10b), eventually connected to hydrophobic aggregates above the cac (Figure 10c). Since the drainage is continuous, we came to the conclusion that the films do not present a semiordered structure. Below the cac , the film thickness is controlled by the size of the self-screened Gaussian coil of the polyelectrolyte, and consequently, a dependence of the thickness with the backbone molecular weight is observed. The counterion osmotic pressure is responsible for the important thickness of the charged polymer films. The film thickness of the corresponding neutral polymer (HMPAAH) is much thinner and is not dependent on the molecular weight. Consequently, it seems that almost all the hydrophobic moieties are adsorbed and that their adsorption energy controls the adsorption of the neutral polymers. Our observations suggest the formation of a neutral monomer brush stretching between the successive anchored grafts in a direction perpendicular to the surface (Figure 9). Consequently, the energy terms which control the organization of the chains ($M_w \geq 34\,000$, $\tau < 10\%$) within the films can be classified in decreasing order of importance

as follows: counterion osmotic pressure > adsorption energy of the grafts > monomer osmotic pressure.

Second, the amphiphilic poly(sodium acrylate)s with lower M_w ($\leq 34\,000$) and higher degree of modification ($\geq 10\%$) form films with a semioordered structure (Figure 10a (●)), the chains being preferentially located in planes parallel to the walls (Figure 10d). The thickness jumps observed during the drainage reveal the presence of an oscillating concentration profile of electrostatic origin with an oscillation wavelength of the order of the mesh size ξ . As mentioned in the Introduction, similar features have already been reported for surfactants and polyelectrolyte mixed films, and they were interpreted in the same manner.^{6–9} The originality of our results is twofold. First, the semioordered structure is observed with films made of a single type of macromolecule in contrast to mixed films. The HMPAANA chains are submitted to a hydrophobic attraction from the walls. The amphiphilic charged polymer chains form both the walls and the inner semioordered structure of the film. Second, the thickness jumps are usually observed with small-size horizontal films submitted to an increasing pressure (typically from 50 to 500 Pa) using a force balance apparatus.^{6–9} In our system, they interestingly occur during the vertical drainage of free-standing macrofilms of several square centimeters, the hydrostatic pressure (100 Pa for a film of 1 cm high) being sufficient to induce the crossover of the successive energy barriers. As for future, we are aware that further experiments are required to understand the existence of the two different types of behavior of HMPAANA films (Figure 10). In particular, it is essential to determine the properties and characteristics of the transition between the two regimes (boundary line in Figure 10). It is also important to keep in mind that the 5.8 25C8Na, 18 20C12Na, and 34 10C12Na copolymers are associative and form hydrophobic intramolecular aggregates in bulk in the range of investigated concentrations.²⁸ Consequently, the thickness jumps could also be due to the presence of charged spherical aggregates in electrostatic interaction. As a matter of fact, films composed of a stratification of spherical micelles of small molecular weight surfactants have already been observed.³⁹ Fluorescent experiments should be useful to test the eventual presence of hydrophobic cores within the films in the case of copolymers of small molecular weight and high degree of grafting. Finally, eq 7 should be tested in further studies of neutral copolymer films by varying the τ value. A major constraint is the solubility of the neutral copolymer (τ C12H) that imposes a τ value lower than 1%, but a variation of τ between 0.1% and 1% could lead to a test of the Marques–Joanny model and provide a more accurate description of the adsorption phenomenon of neutral random copolymers. A wider range of τ could also be achieved using shorter grafts (C8).

Acknowledgment. The authors thank C. Tribet, who kindly supplied us with the 5.8 25C8Na copolymer. We had very fruitful discussions with O. Mondain-

Monval, I. Iliopoulos, P. Guenoun, A. Khokhlov, S. Obukhov, and M. Rubinstein. The help of N. Cuvillier in the data treatment and the experimental participation of R. Benbalagh were greatly appreciated.

References and Notes

- (1) Millet, F.; Perrin, P.; Benattar, J.-J. *Phys. Rev. E* **1999**, *60*, 2045.
- (2) B lorgey, O.; Benattar, J.-J. *Phys. Rev. Lett.* **1991**, *66*, 373.
- (3) Cuvillier, N.; Millet, F.; Petkova, V.; Nedyalkov, M.; Benattar, J.-J. *Langmuir* **2000**, *16*, 5029.
- (4) Millet, F.; Nedyalkov, M.; Renard, B.; Perrin, P.; Lafuma, F.; Benattar, J.-J. *Langmuir* **1999**, *15*, 2112.
- (5) Carignano, M. A.; Dan, N. *Langmuir* **1998**, *14*, 3475.
- (6) Bergeron, V.; Asnacios, A.; Langevin, D. *Langmuir* **1996**, *12*, 1550.
- (7) Asnacios, A.; Espert, A.; Colin, A.; Langevin, D. *Phys. Rev. Lett.* **1997**, *78*, 4974.
- (8) Klitzing, R. v.; Espert, A.; Asnacios, A.; Hellweg, T.; Colin, A.; Langevin, D. *Colloids Surf.* **1999**, *149*, 131.
- (9) Th  odoly, O. Ph.D. Thesis, Universit   Paris 6, Paris, France, 1999.
- (10) Perrin, P.; Lafuma, F. *J. Colloid Interface Sci.* **1998**, *197*, 317.
- (11) Perrin, P.; Lafuma, F.; Audebert, R. *Prog. Colloid Polym. Sci.* **1997**, *105*, 228.
- (12) Perrin, P. *Langmuir* **1998**, *14*, 5977.
- (13) Perrin, P.; Monfreux, N.; Thierry, F.; Lafuma, F.; Lequeux, F. *Proc. ACS Div. Polym. Mater. Sci. Eng.* **1999**, *81*, 492.
- (14) Perrin, P.; Devaux, N.; Sergot, P.; Lequeux, F. *Langmuir* **2001**, *17*, 2656.
- (15) Wang, T. K.; Iliopoulos, I.; Audebert, R. *Polym. Bull.* **1989**, *20*, 577.
- (16) Born, M.; Wolf, E. *Principles of Optics*; Pergamon: London, 1980.
- (17) Israelachvili, J. N.; Tirell, M.; Klein, J.; Almog, Y. *Macromolecules* **1984**, *17*, 204.
- (18) Klein, J.; Luckham, P. F. *Nature* **1984**, *308*, 836.
- (19) Dahlgren, M. A. G.; Waltermo, A.; Blomberg, E.; Claesson, P. M.; S  jstr  m, L.;   kesson, T.; J  nsson, B. *J. Phys. Chem.* **1993**, *97*, 11769.
- (20) Dahlgren, M. A. G.; Claesson, P. M.; Audebert, R. *J. Colloid Interface Sci.* **1994**, *166*, 343.
- (21) Rojas, O. J.; Claesson, P. M.; Muller, D.; Neuman, R. D. *J. Colloid Interface Sci.* **1998**, *205*, 77.
- (22) Klein, J. *Nature* **1980**, *288*, 248.
- (23) Derjaguin, B. V.; Landau, L. *Acta Physicochim. URSS* **1941**, *14*, 633.
- (24) Verwey, E. J. W.; Overbeek, J. T. G. *Theory of Stability of Lipophilic Colloids*; Elsevier: Amsterdam, 1948.
- (25) de Gennes, P.-G.; Pincus, P.; Velasco, R. M.; Brochard, F. *J. Phys. (Paris)* **1976**, *37*, 1461.
- (26) Odijk, T. *Macromolecules* **1979**, *12*, 688.
- (27) Khokhlov, A. R.; Khachatryan, K. A. *Polymer* **1982**, *23*, 1742.
- (28) Petit, F. Ph.D. Thesis, Universit   Paris 6, Paris, France, 1996.
- (29) Barrat, J.-L.; Joanny, J.-F. *Adv. Chem. Phys.* **1996**, *XCIV*, 1.
- (30) Manning, G. S. *J. Chem. Phys.* **1969**, *51*, 924.
- (31) Dobrynin, A. V.; Colby, R. H.; Rubinstein, M. *Macromolecules* **1995**, *28*, 1859.
- (32) de Gennes, P.-G. *Scaling Concepts in Polymer Physics*; Cornell University Press: Ithaca, NY, 1979.
- (33) Essafi, W.; Lafuma, F.; Williams, C. E. Macro-Ion Characterization from Dilute Solutions to Complex Fluids. *ACS Symp. Ser.* **1993**, *548*, 278.
- (34) Pincus, P. *Macromolecules* **1991**, *24*, 2912.
- (35) Wittmer, J.; Joanny, J.-F. *Macromolecules* **1993**, *26*, 2691.
- (36) Guenoun, P.; Schalchli, A.; Sentenac, D.; Mays, J. W.; Benattar, J.-J. *Phys. Rev. Lett.* **1995**, *74*, 3628.
- (37) Alexander, S. *J. Phys. (Paris)* **1977**, *38*, 983.
- (38) Marques, C. M.; Joanny, J.-F. *Macromolecules* **1990**, *23*, 268.
- (39) Bergeron, V.; Radke, C. J. *Langmuir* **1992**, *8*, 3020.

MA001742F